

Electrocatalytic Oxidation of Guanine and Adenine Based on Iron Hexacyanoferrate Film Modified Electrodes

Shen-Ming Chen*, Ching-Hung Wang, Kuo-Chiang Lin

Electroanalysis and Bioelectrochemistry Lab, Department of Chemical Engineering and Biotechnology, National Taipei University of Technology, No.1, Section 3, Chung-Hsiao East Road, Taipei 106, Taiwan (ROC).

*E-mail: smchen78@ms15.hinet.net

Received: 9 November 2011 / Accepted: 12 December 2011 / Published: 1 January 2012

Iron hexacyanoferrate (FeHCF) film was successfully prepared on electrode surface in the mixing Fe^{3+} and $\text{Fe}(\text{CN})_6^{3-}$ solution and studied with two monovalent cations (K^+ and Na^+) by consecutive cyclic voltammetry. The growth mechanism of FeHCF film was studied by cyclic voltammetry with an electrochemical quartz crystal microbalance (EQCM). The results indicated that the FeHCF confined to the electrode surface. EQCM results showed ion exchange reaction of K^+ and Na^+ to the correlative redox couples. The electrocatalytic oxidation of guanine, adenine, and their mixture by FeHCF film was accomplished and it showed different electrocatalytic properties in K^+ and Na^+ aqueous solutions. The electrocatalytic oxidation of NADH, dopamine, L-cysteine, N_2H_4 and NH_2OH was investigated as well as the electrocatalytic reduction of H_2O_2 . Moreover, the electrocatalytic reaction of dopamine was also investigated by FeHCF film using the rotating ring-disk electrode method. Linear concentration range of 0–145 μM was found for guanine with sensitivity of 1818 $\mu\text{A mM}^{-1} \text{cm}^{-2}$ and detection limit of 0.1 μM (S/N = 3).

Keywords: Guanine, Adenine, Film modified electrodes, Hexacyanoferrate, Electrocatalysis, Biosensors, Bioelectrochemistry, DNA, Electrochemistry

1. INTRODUCTION

Investigations of the redox behavior of the biologically occurring compounds by means of electrochemical techniques have the potential for providing valuable insights into biological redox reactions of such biomolecules. Since the electroactivity of deoxyribonucleic acid (DNA) was discovered [1], there have been intensive efforts to apply modern electrochemical methods in nucleic acid research and DNA analysis [2]. Modern electrochemical techniques and related methodologies provide the most powerful approaches to elucidating mechanistic information concerning redox

reactions. Because guanine (G) is the most easily oxidized nitrogenous base, the chemical mechanism of its oxidation has been studied in detail [3,4]. While the mechanism of G and adenine (A) oxidation in solution has been well investigated, there have been very few mechanistic studies of the oxidation of these analytes at the surface of an electrode. This information would be useful for the design of electrochemical nucleic acid biosensors based on the detection of G and A oxidation [5,6].

Electrochemistry of nucleic acids is booming due to the development of electrochemical transducer-based devices for diagnosing, preventing and treating many human diseases [7-9]. The electrochemical oxidation mechanisms of G and A were investigated along with their relevance to oxidative degradation of nucleic acids in mutagenesis, carcinogenesis, and aging. Determining individual concentrations of G and A or their ratio in DNA is important for the measurement of nucleic acid concentration itself. Measurement of the electron-transfer of G in solution is important and helpful in understanding the oxidation processes of DNA [10-14]. $[\text{Ru}(\text{bpy})_3]^{2+}$ has been performed to the electrocatalytic G oxidation [15,16]. Ruthenium-tris(2, 2-bipyridyl)dichloro-ruthenium(II) modified carbon paste electrode was used for electrocatalytic detection of DNA [13]. Mikkelsen and coworkers detected DNA on carbon electrodes by immobilizing the DNA onto the electrode and then measuring the enhanced Faradaic current of $\text{Co}(\text{bpy})_3^{2+/3+}$ in the presence of the surface attached DNA. In addition, numerous methods for attaching DNA to electrode materials have been described [2, 17–20]. The electrochemical study of nucleic acids and their adsorption on different types of electrode materials has recently been of great interest [21]. These nucleobase oxidations have been observed when they are adsorbed onto carbon paste electrodes. Wang et al. have focused on the detection of direct oxidation of the G and A bases adsorbed on carbon electrodes [6, 18, 22, 23]. In addition, Kuhr et al. have achieved a sensitive detection system based upon catalytic oxidation of the deoxyribose (or ribose) sugar in nucleic acid at a copper microelectrode [24,25]. Our laboratory has also recently developed the use of chemically (mainly transition metal hexacyanoferrates as electrontransfer mediators) modified carbon paste electrodes for enhancing the voltammetric response of G, DNA and other biologically important analytes [26].

Metal hexacyanoferrates show interesting redox chemistry that is used in both chemistry and materials science. Chemically modified film electrodes of metal hexacyanoferrates [27–35] show interesting redox properties, such as in electroanalysis, chemical sensing and electrocatalysis [36–44].

The results of the electrocatalytic activity measurements on the Metal hexacyanoferrate film are useful to analytical applications, and to the electrochemical reaction transfer activity of low electroactive compounds. The analytical methods used are well established, and they are important for the determination of these analytes.

This paper reports on the successful preparation of FeHCF film formed by directly mixing Fe^{3+} and $\text{Fe}(\text{CN})_6^{3-}$, and deposited onto a working electrode in Na^+ , K^+ monovalent cation electrolyte solutions by consecutive cyclic voltammetry. It showed two and three redox couples in K^+ and Na^+ aqueous solutions, respectively. Electrochemical quartz crystal microbalance (EQCM) and cyclic voltammetry were used to study the in situ growth processes of the FeHCF film, their electrochemical properties, and ion exchange properties. The electrocatalytic oxidation of guanine, adenine, and their mixture showed selectively electrocatalytic activity in K^+ and Na^+ cation aqueous solution, respectively. The experiments were carried out in the electrocatalytic oxidation of NADH, dopamine,

L-cysteine, N_2H_4 , and NH_2OH , as well as the electrocatalytic reduction of H_2O_2 using FeHCF film modified electrodes. Moreover, the electrocatalytic reaction of dopamine was investigated by the FeHCF film through the rotating ring-disk electrode method.

2. EXPERIMENTAL

The electrochemistry was performed by a Bioanalytical Systems Model CV-50W, a CH Instruments CHI-400, and a CHI-750 potentiostats. Cyclic voltammetry was conducted using a three-electrode cell in which a BAS glassy carbon electrode, a platinum electrode, and an indium tin dioxide (ITO) electrode were used as the working electrodes. The glassy carbon electrode was polished with 0.05 μm alumina on Buehler felt pads, and then ultrasonically cleaned in doubly distilled deionized water for 1 min. The auxiliary compartment contained a platinum wire, which was separated by a medium-sized glass frit. All cell potentials were taken using an Ag/gCl (with saturated KCl solution) reference electrode.

The working electrode for the EQCM measurements was an 8 MHz AT-cut quartz crystal with gold-coated electrode. The diameter of the quartz crystal was 13.7 mm and the gold electrode diameter was 5 mm.

The RRDE experiments were performed using a ring-disk electrode (Pine Instrument Co.) in conjunction with a CH Instruments CHI-750 potentiostat connected to a model AFMSRX analytical rotator. The rotating ring-disk electrode (RRDE), purchased from the Pine Instrument Co., consisted of a glassy carbon disk electrode and a glassy carbon (or platinum) ring electrode.

All the chemicals used were of analytical grade. The $K_3Fe(CN)_6$ and $FeCl_3$ were purchased from the Aldrich Chemical Co., USA. NADH and dopamine were purchased from the Sigma Chemical Co., USA. The aqueous solutions were prepared using doubly distilled deionized water, and the solutions were deoxygenated by purging with pre-purified nitrogen gas.

3. RESULTS AND DISCUSSION

3.1. Preparation of FeHCF film in KCl and NaCl aqueous solutions

The electrochemical formation of FeHCF film was carried out on a glassy carbon electrode by consecutive cyclic voltammetry. Potassium chloride and sodium chloride were individually chosen as the electrolyte when using a glassy carbon electrode to study the FeHCF film formation.

Fig. 1A showed the consecutive cyclic voltammograms of FeHCF film deposited on electrode surface in 0.1 M KCl aqueous solution (pH 6) containing 10^{-3} M Fe^{3+} and 10^{-3} M $Fe(CN)_6^{3-}$. Two redox couples were found with the formal potential of +0.14 V and +0.82 V. The former was easily recognized by comparison with the $Fe^{III}(CN)_6^{3-}/Fe^{II}(CN)_6^{4-}$ redox process (shown in the curve a' of Fig. 1A) while the latter was expressed as the $Fe^{III}Fe^{III}(CN)_6/KFe^{II}Fe^{III}(CN)_6$ redox process. Inset a & b showed that the anodic peak currents (relate to two redox couples) were increasing with the increase of

scan cycles. The bending curve means that the film was deposited on electrode surface and it was approaching to the deposition limit.

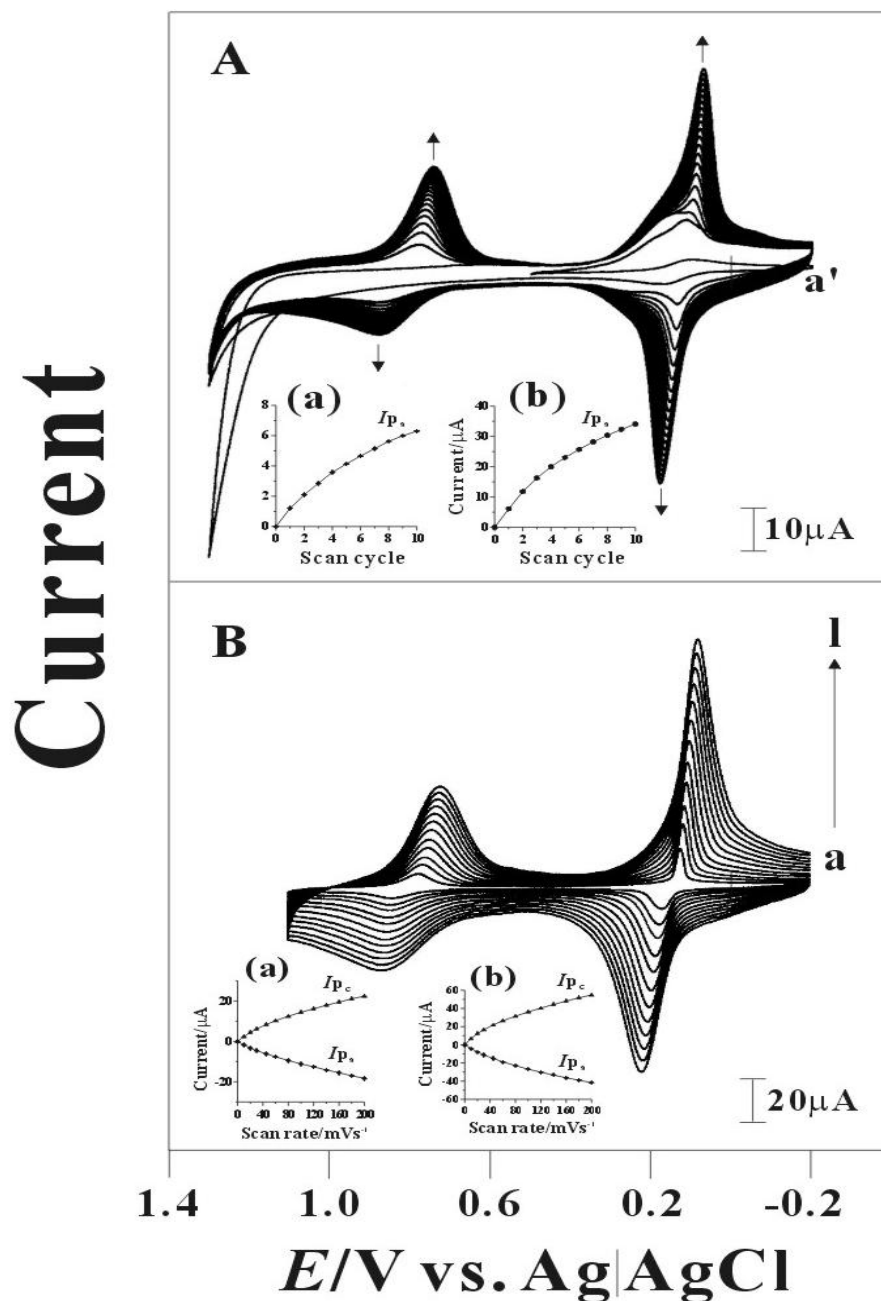


Figure 1. (A) Repetitive cyclic voltammograms of iron(III) hexacyanoferrate (FeHCF) deposited on a glassy carbon electrode in 0.1 M KCl aqueous solution containing 1×10^{-3} M Fe^{3+} and 1×10^{-3} M $\text{Fe}(\text{CN})_6^{3-}$. (a') Cyclic voltammogram of a glassy carbon electrode examined in 0.1 M KCl aqueous solution containing 1×10^{-3} M $\text{Fe}(\text{CN})_6^{3-}$. Scan rate = 0.1 Vs^{-1} . Insets: the anodic peak current (I_{pa}) vs. scan cycle at (a) $E_{pa} = 0.88$ V and (b) $E_{pa} = 0.18$ V, respectively. (B) Cyclic voltammograms of FeHCF/GCE examined in 0.1 M KCl aqueous solution with scan rate of: (a) 0.01, (b) 0.02, (c) 0.03, (d) 0.045, (e) 0.06, (f) 0.08, (g) 0.1, (h) 0.12, (i) 0.14, (j) 0.16, (k) 0.18, and (l) 0.2 Vs^{-1} , respectively. Insets: the plot of the peak currents (I_{pc} & I_{pa}) vs. scan rate at (a) $E^{0'} = 0.8$ V and (b) $E^{0'} = 0.15$ V, respectively.

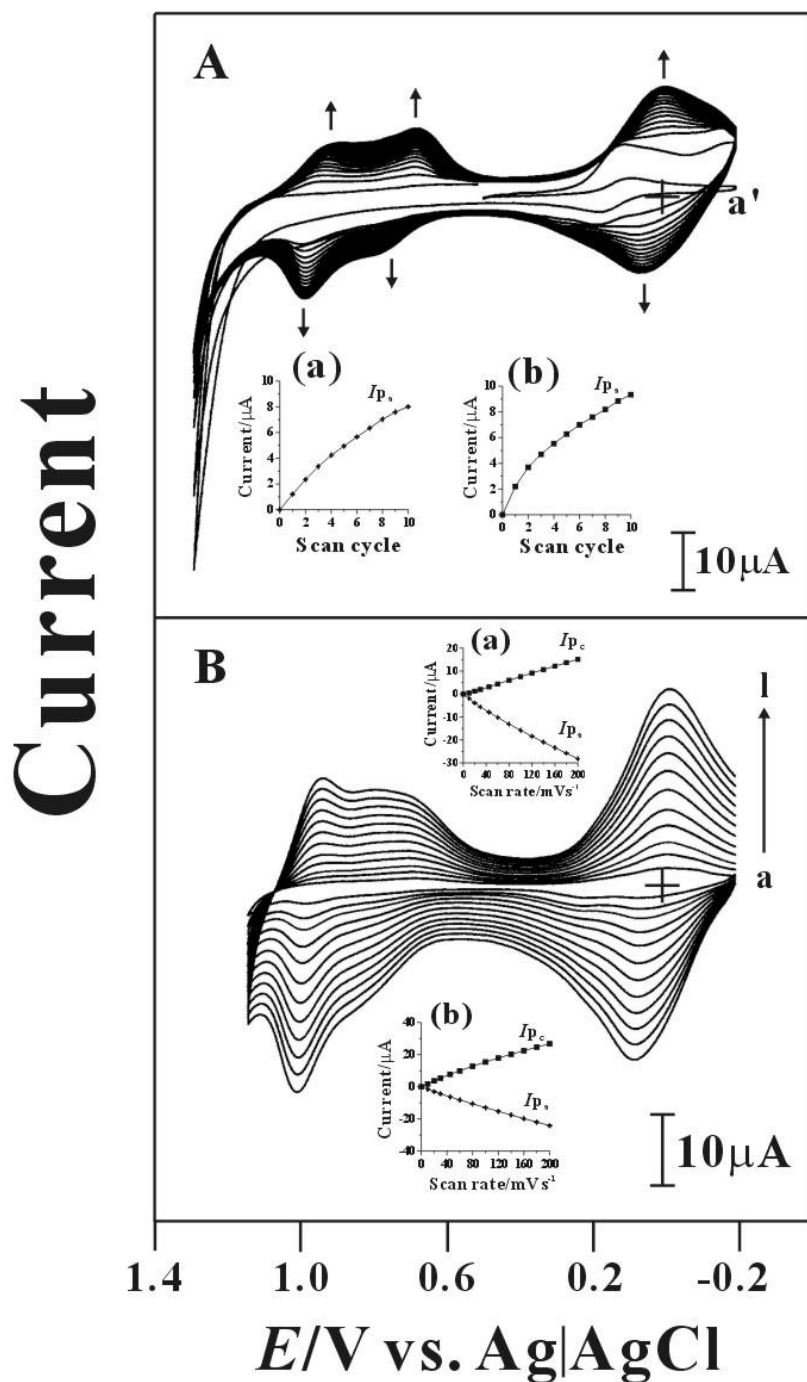


Figure 2. (A) Repetitive cyclic voltammograms of iron(III) hexacyanoferrate (FeHCF) deposited on a glassy carbon electrode in 0.1 M NaCl aqueous solution containing 1×10^{-3} M Fe^{3+} and 1×10^{-3} M $\text{Fe}(\text{CN})_6^{3-}$. (a') Cyclic voltammogram of a glassy carbon electrode examined in 0.1 M NaCl aqueous solution containing 1×10^{-3} M $\text{Fe}(\text{CN})_6^{3-}$. Scan rate = 0.1 V s^{-1} . Insets: the anodic peak current (I_{pa}) vs. scan cycle at (a) $E_{pa} = 1.0 \text{ V}$; (b) $E_{pa} = 0.82 \text{ V}$. (c) the anodic peak current (I_{pa}) vs. scan cycle at $E_{pa} = 0.06 \text{ V}$. (B) Cyclic voltammograms of FeHCF/GCE examined in 0.1 M NaCl aqueous solution with scan rate of: (a) 0.01, (b) 0.02, (c) 0.03, (d) 0.045, (e) 0.06, (f) 0.08, (g) 0.1, (h) 0.12, (i) 0.14, (j) 0.16, (k) 0.18, and (l) 0.2 V s^{-1} . Insets: the peak currents (I_{pc} & I_{pa}) vs. scan rate at (a) $E^{0'} = 0.97 \text{ V}$ and (b) $E^{0'} = 0.77 \text{ V}$, respectively. (c) the peak currents I_{pc} vs. scan rate and I_{pa} vs. scan rate at $E^{0'} = 0.03 \text{ V}$.

The film was further tested in the blank solution containing potassium chloride. Fig. 1B showed that the cyclic voltammograms of FeHCF/GCE examined with various scan rates in 0.1 M KCl solution. It exhibited two reversible redox couples and the current was increasing with the increase of scan rate. Inset a & b showed the plots of the peak current (I_{pa} and I_{pc}) versus scan rate for two redox couples, respectively. It resulted in a close linear dependence of peak current (I_p) on the scan rate and the I_{pa}/I_{pc} ratio was approximately equal to 1. This result indicated that the redox process was confined to the surface of the FeHCF film on the glassy carbon electrode, confirming the immobilized state of the FeHCF [45–47].

The investigation of FeHCF film formation was also studied with the different supporting electrolyte. Here, sodium chloride was chosen as supporting electrolyte to take consecutive cyclic voltammograms and compared with those used in potassium chloride. Fig. 2A showed the consecutive cyclic voltammograms of FeHCF deposited on electrode surface in 0.1 M NaCl solution (pH 6) containing Fe^{3+} and $Fe(CN)_6^{3-}$. In this case, three group redox couples were found with the formal potential of +0.04 V, +0.76 V, and +0.95 V. The former two were similar to those in potassium chloride. Particularly, one redox couple appeared in the more positive potential. This might be due to the different composite of FeHCF made by different supporting electrolytes. The cations of K^+ and Na^+ might exchange in composite when FeHCF prepared in different electrolytes containing different cations.

Various scan rates were tested as Fig. 2B, inset a & b showed the plots of cathodic and anodic peak current (I_{pc} & I_{pa}) versus scan rate, illustrating a close linear dependence of I_{pc} & I_{pa} on the scan rate, and that the anodic to the cathodic peak current ratio (I_{pa}/I_{pc}) was equal to 1. This result was also consistent with diffusion-less, reversible electron transfer process at low scan rates. The peak current and scan rate were related as follows [45–47]:

$$I_p = n^2 F^2 v A \Gamma_o / 4RT \quad (1)$$

where, Γ_o , v , A , and I_p represent the surface coverage concentration, the scan rate, the electrode area, and the peak current, respectively.

3.2. FeHCF film formation studied by in-situ EQCM measurements and potential-switching chronoamperometry

In the EQCM experiments, the change in mass (or coverage) at the quartz crystal was calculated from the change in the observed frequency using the Sauerbrey equation [48,49]. The film coverage (unit: $ng\ cm^{-2}$ or $mole\ cm^{-2}$) deposited on the electrode's surface during the electrochemical process can be calculated as following equation:

$$\text{Mass change } (\Delta m) = (-1/2)(f_o^{-2})(\Delta f)A(k\rho)^{1/2} \quad (2)$$

where A is the area of the gold disk coated onto the quartz crystal, ρ is the density of the crystal, k is the shear modulus of the crystal, Δf is the measured frequency change, and f_0 is the oscillation frequency of the crystal. A frequency change of 1 Hz is equivalent to a 1.4 ng change in mass.

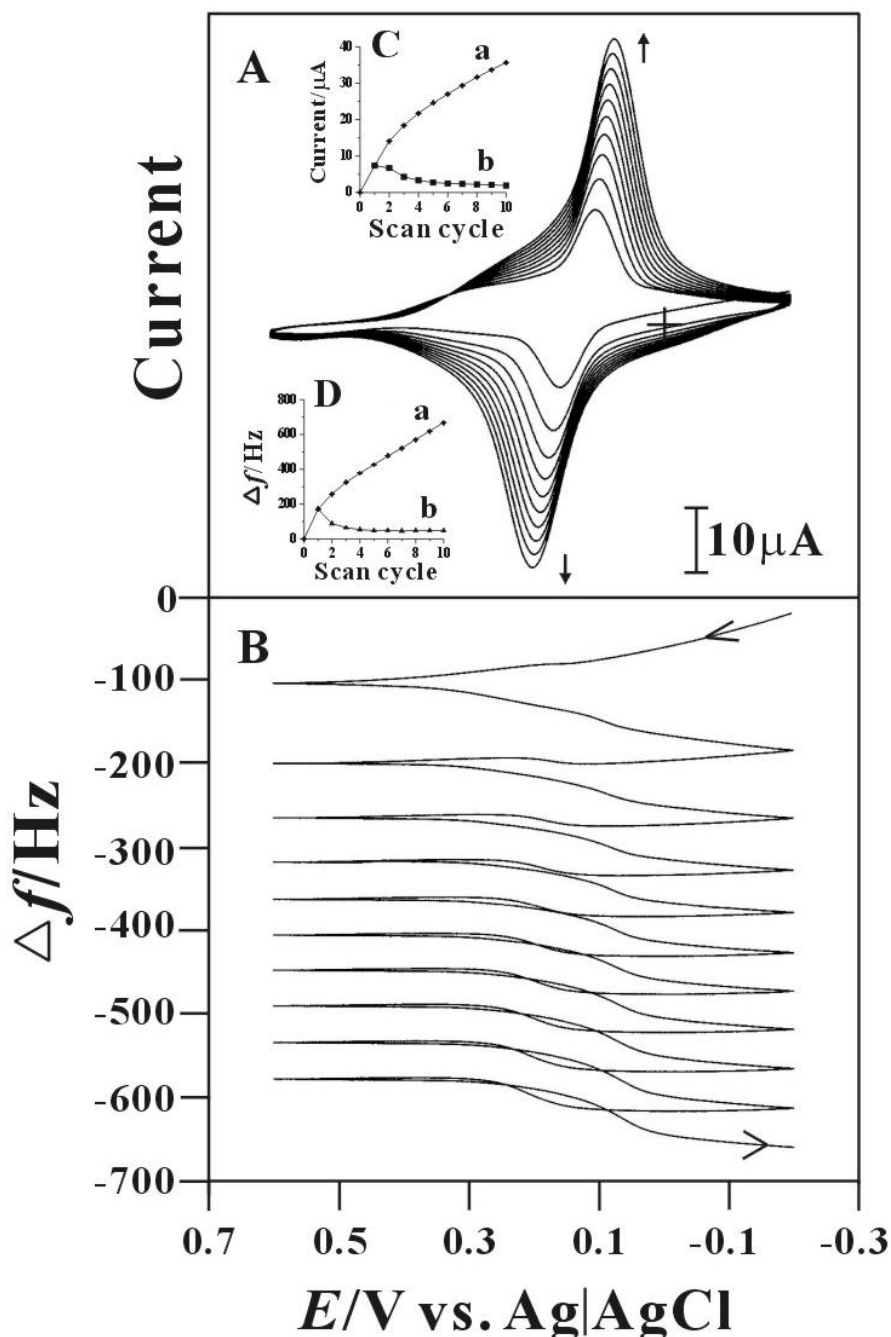


Figure 3. (A) Consecutive cyclic voltammograms of FeHCF film synthesized in the 0.1 M KCl containing 1×10^{-3} M Fe^{3+} and 1×10^{-3} M $\text{Fe}(\text{CN})_6^{3-}$. Electrode: gold-coated quartz. Scan rate: 0.02 V s^{-1} . (B) EQCM frequency change recorded concurrent with the first ten consecutive cyclic voltammogram cycles between -0.2 V and 0.6 V. Insets: the plots of (C) peak current (I_{pa}) and (D) frequency change (Δf) vs. scan cycle, respectively. Curve (a) means for total current or total frequency change and (b) means for net current or net frequency vs. scan cycle, respectively.

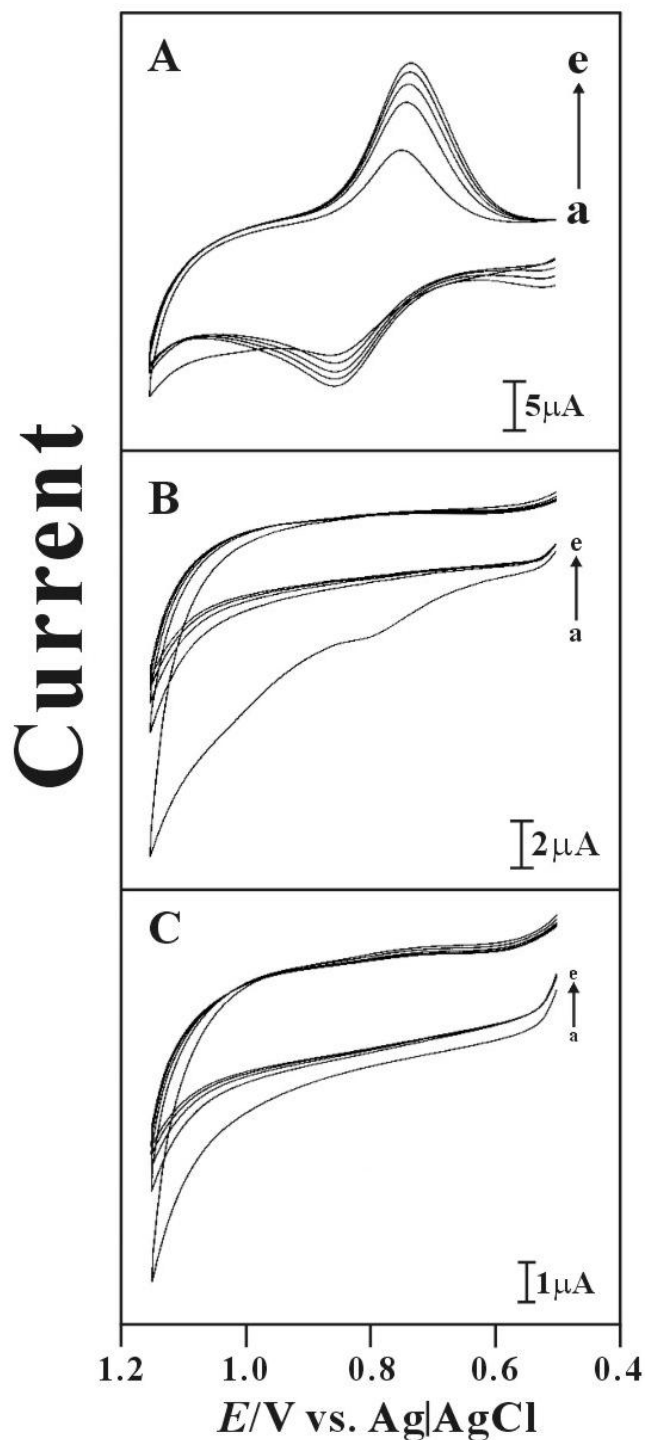


Figure 4. Cyclic voltammograms of a glassy carbon electrode examined in 0.1 M KCl aqueous solution containing 1×10^{-3} M Fe^{3+} and 1×10^{-3} M $\text{Fe}(\text{CN})_6^{3-}$ after chronoamperometry with different pulse potentials: (A) -0.2 V, (B) +0.65 V, (C) +1.15 V (vs. Ag/AgCl) and different durations: (a) 0 s, (b) 2 s, (c) 4 s, (d) 6 s, and (e) 8 s, respectively. Scan rate = 0.1 V s^{-1} .

FeHCF film was successfully deposited on a gold electrode in 0.1 M KCl solution (pH 6). Fig. 3A recorded the voltammetric response of FeHCF deposition while Fig. 3B recorded the EQCM frequency change of FeHCF film deposited on the gold electrode in the same time. The frequency

change resulting in the deposited amount. The potential range was set in the range of $-0.2 \sim 0.6$ V to observe the correlation between voltammogram and frequency change. One redox couple with formal potential at approximately $+0.1$ V was found in the voltammogram (Fig. 3A). Fig. 3B showed the EQCM frequency change during the first ten scan cycles by consecutive cyclic voltammetry. The frequency change varied strictly at $+0.1$ V, it means that the film formation involved the $\text{Fe}^{\text{III}}(\text{CN})_6^{3-}/\text{Fe}^{\text{II}}(\text{CN})_6^{4-}$ redox process. The deposition occurred between 0.3 V and -0.2 V. In this potential range, $\text{Fe}^{\text{III}}(\text{CN})_6^{3-}$ was reduced to $\text{Fe}^{\text{II}}(\text{CN})_6^{4-}$, the Fe^{2+} and $\text{Fe}^{\text{II}}(\text{CN})_6^{4-}$ simultaneously reacted to form a new species and deposited on the electrode surface. In the first scan cycle, approximately 1430 ng cm^{-2} of FeHCF was deposited on the gold electrode. Approximately 4790 ng cm^{-2} of FeHCF was deposited on the gold electrode after ten scan cycles. The inset C showed a plot of the cathodic peak current change versus scan cycle, and the inset D showed the total frequency change versus scan cycle. By the result, it was obviously to see the relatively large electro-deposition amount by the first scan cycle with large frequency change. From the frequency change result (shown in Fig. 3B), the deposition amount was getting less in the later scan cycles.

The effect of potential-switching for FeHCF film deposition was further studied in the potential range $+0.5$ to $+1.15$ V by cyclic voltammetry. Fig. 4A-C showed the cyclic voltammograms recorded after chronoamperometry applied potential of -0.2 V, $+0.65$ V, $+1.15$ V with different durations of (a) 0 s, (b) 2 s, (c) 4 s, (d) 6 s, and (e) 8 s, respectively. By the result, the obvious anodic and cathodic peak currents drastically increased only with the potential-switching at -0.2 V. This means that the $\text{Fe}^{\text{III}}(\text{CN})_6^{3-}$ reduced to $\text{Fe}^{\text{II}}(\text{CN})_6^{4-}$, Fe^{3+} reduced to Fe^{2+} , and $\text{Fe}^{\text{II}}(\text{CN})_6^{4-}$ reacted with Fe^{2+} favors at this potential ($E_{\text{app.}} = -0.2$ V), thereby increasing the film yield. On contrary, potential applied at $+1.15$ V and $+0.65$ V even with long duration time can't drive the cathodic and anodic peak currents develop to form the film. Therefore, one can conclude that the film formation involved a key potential step of reduction.

3.3. Ion exchange effect of FeHCF film

FeHCF film was examined with different monovalent cations in 0.1 M KCl and 0.1 M NaCl, respectively. Fig. 5A & C showed the results of cyclic voltammetry and EQCM measurements of FeHCF film examined in K^+ and Na^+ solutions, respectively. In the potential range of -0.3 to 0.6 V, Fig. 5A(a) & (b) showed that the one redox couple and frequency change, respectively. The frequency increase (or mass decrease) in Fig. 5A was consistent with a K^+ ion exchange related to the redox couple.

The kinetics of the potential-switching response of FeHCF film in KCl to assess its performance as a display device was investigated. Fig. 5B showed the results for potential-switching between -0.2 V and 0.6 V. In these experiments, a square wave potential was applied over a 2 s period to assess the film with cations exchange. The cations exchange phenomena can be also observed in the Na^+ system as the result in Fig. 5C & D. The FeHCF film was found with good reversibility during the potential cycling and the cations (K^+ and Na^+) exchange was also found obviously in the frequency change related to the redox couple.

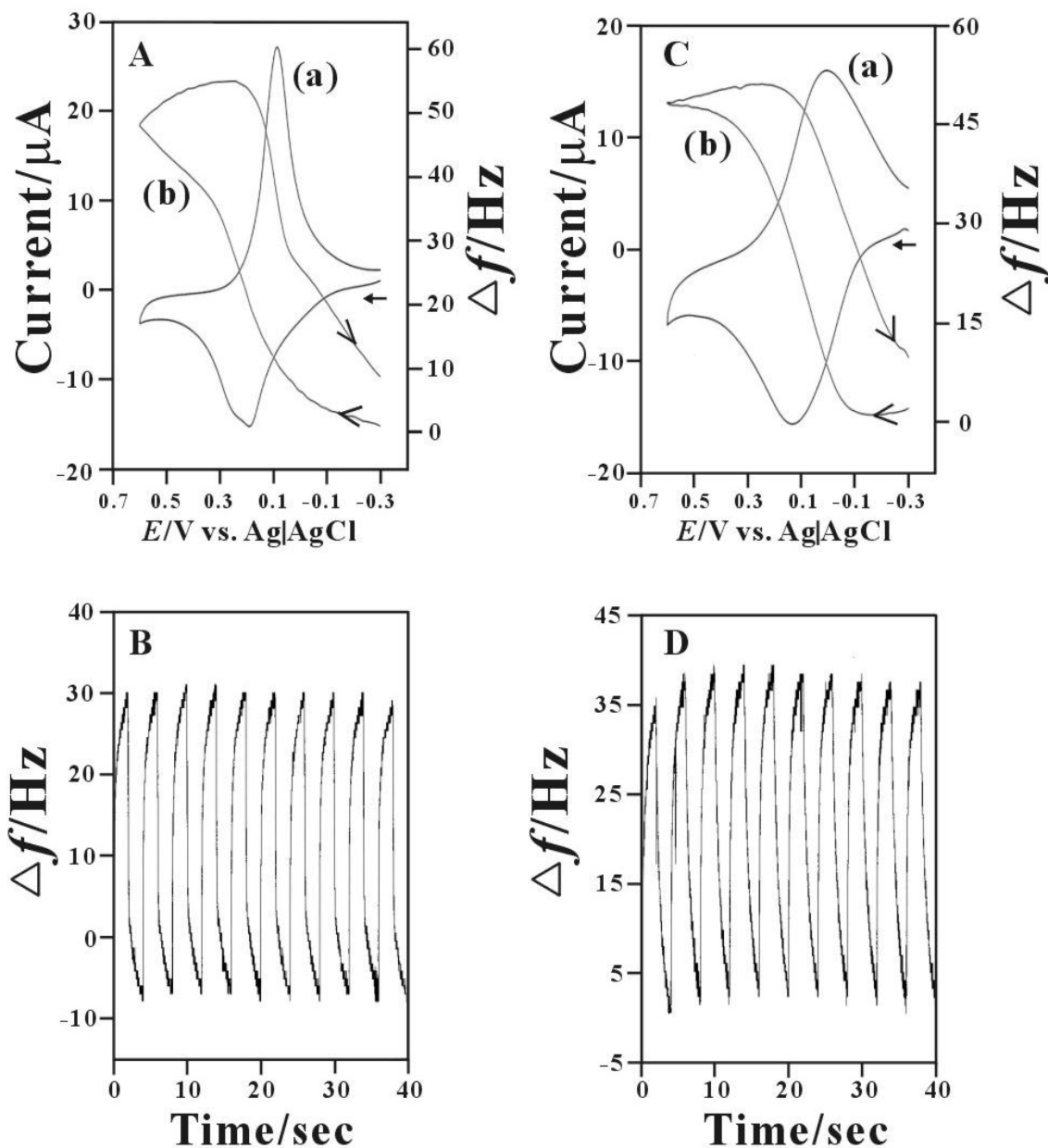


Figure 5. (A) (a) Cyclic voltammograms of FeHCF/GCE in 0.1 M KCl aqueous solution. (b) Microgravimetric frequency change of FeHCF/AUE in 0.1 M KCl aqueous solution. Scan rate = 0.02 V s^{-1} . (B) EQCM measurements of FeHCF/AUE in 0.1 M KCl aqueous solution during potential switching from $E_{\text{app.}} = -0.2$ to 0.6 V (vs. Ag/AgCl) using a time pulse of 2 s. (C) (a) Cyclic voltammograms of FeHCF/GCE in 0.1 M NaCl aqueous solution. (b) Microgravimetric frequency change of FeHCF/AUE in 0.1 M NaCl aqueous solution. Scan rate = 0.02 V s^{-1} . (D) EQCM measurements of FeHCF/AUE in 0.1M NaCl aqueous solution during potential switching from $E_{\text{app.}} = -0.2$ to 0.6 V (vs. Ag/AgCl) using a time pulse of 2 s.

The electrochemical behavior of FeHCF film with potential-switching was also studied by chronoamperometry. The potential-switching from $+0.5 \text{ V}$ to -0.2 V and from $+0.5 \text{ V}$ to $+1.15 \text{ V}$ were individually tested and compared on FeHCF film in KCl or NaCl solution. In these experiments, a square wave potential was applied over a period of 2 s during oxidation-reduction process. Fig. 6A &

B showed the chronoamperograms for $\text{K}_3\text{Fe}^{\text{III}}(\text{CN})_6/\text{K}_4\text{Fe}^{\text{II}}(\text{CN})_6$ and $\text{KFe}^{\text{II}}\text{Fe}^{\text{III}}(\text{CN})_6/\text{Fe}^{\text{III}}\text{Fe}^{\text{III}}(\text{CN})_6$ redox processes in potential-switching of +0.5 V to -0.2 V and +0.5 V to +1.15 V, respectively.

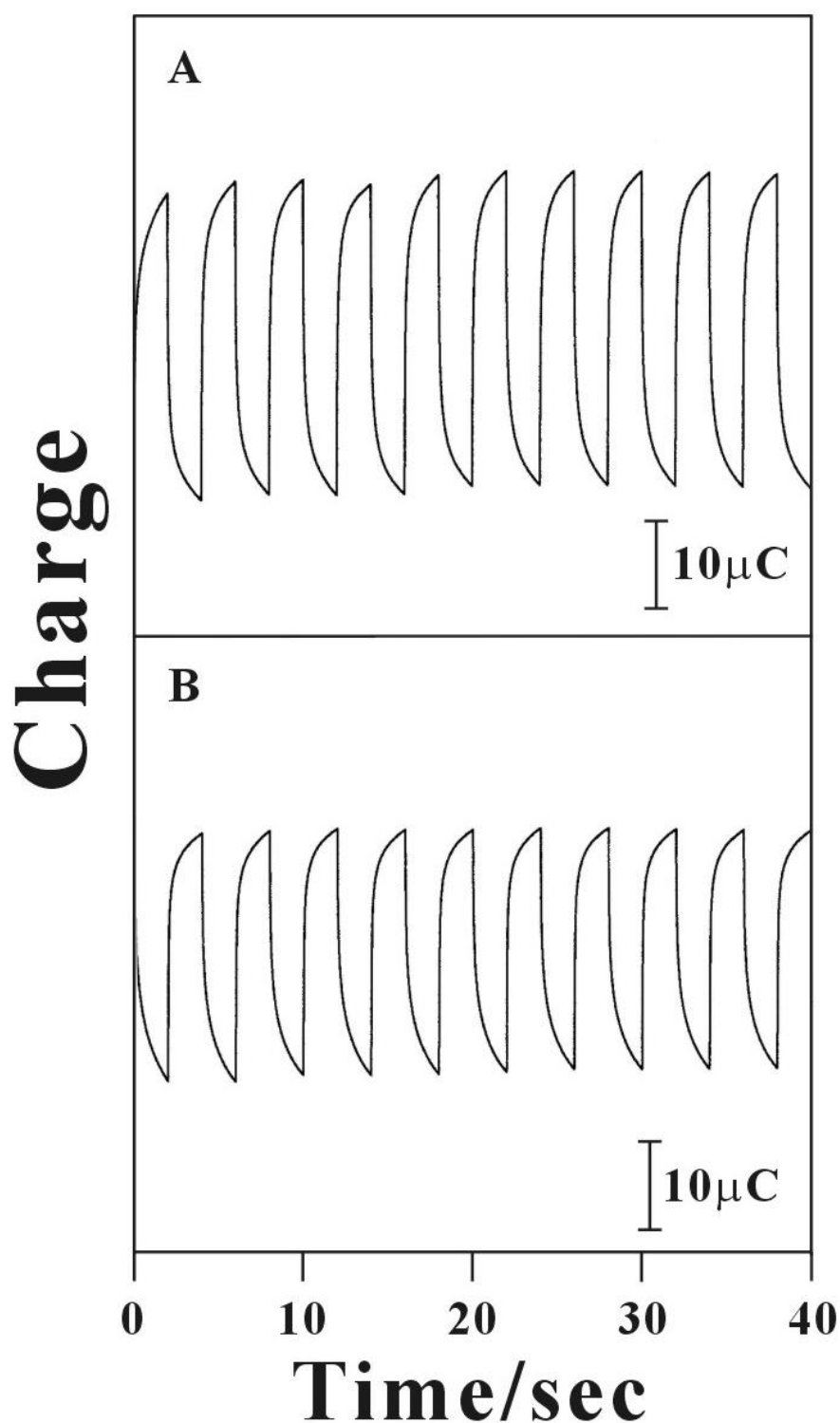


Figure 6. Chronocoulometry of FeHCF/GCE in the 0.1 M KCl aqueous solution during potential switching from: (A) $E_{\text{app}} = +0.5 \text{ V}$ to -0.2 V (vs. Ag/AgCl); (B) $E_{\text{app}} = +0.5 \text{ V}$ to $+1.15 \text{ V}$ (vs. Ag/AgCl).

It exhibited the significant peak with repeatable amplitude in the period. It means that the reversibility of FeHCF film was consistent with charge change and the K^+ ion exchange occurrence was confirmed.

3.4. Electrocatalytic oxidation of guanine and adenine in KCl and NaCl aqueous solutions by FeHCF film

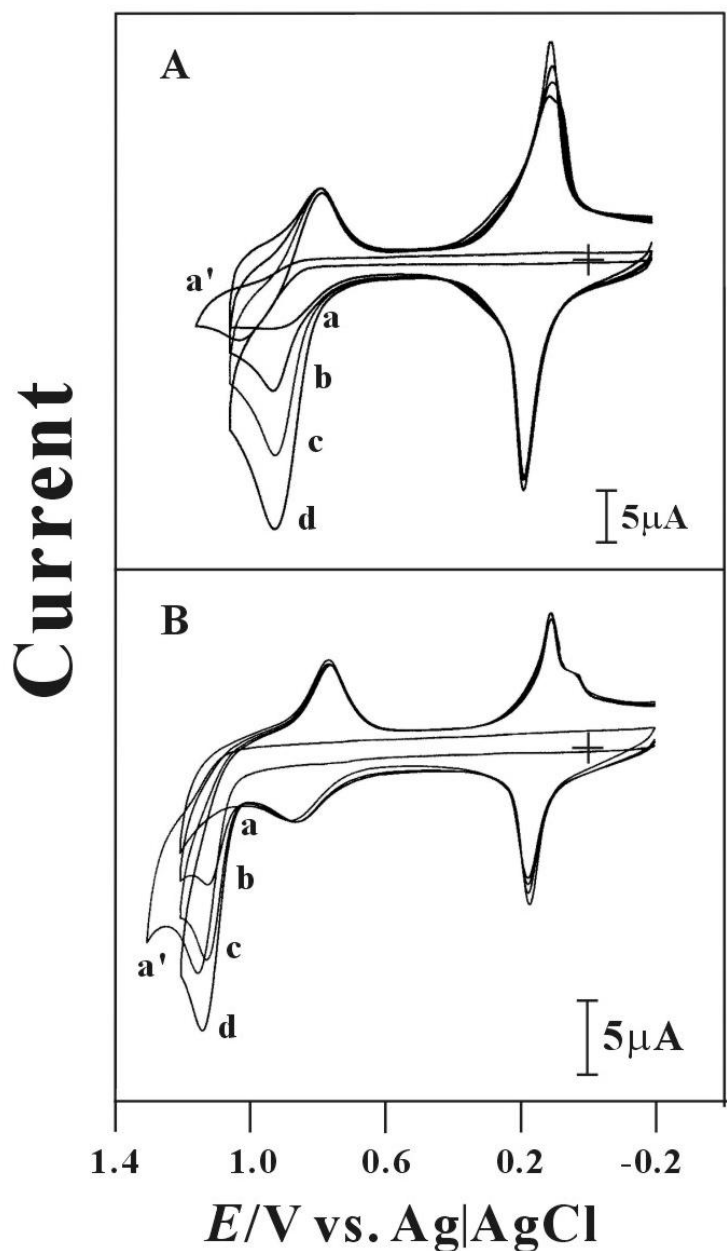


Figure 7. Cyclic voltammograms of FeHCF/GCE examined in 0.1 M KCl aqueous solution with: (A) [guanine]: (a) 0, (b) 1.5×10^{-3} , (c) 3×10^{-3} , (d) 4.5×10^{-3} M; and (B) [adenine]: (a) 0, (b) 1×10^{-3} , (c) 2×10^{-3} M and (d) 3×10^{-3} M, respectively. (a') Bare glassy electrode examined with maximal reagent addition in each case. Scan rate = 0.1 V s^{-1} .

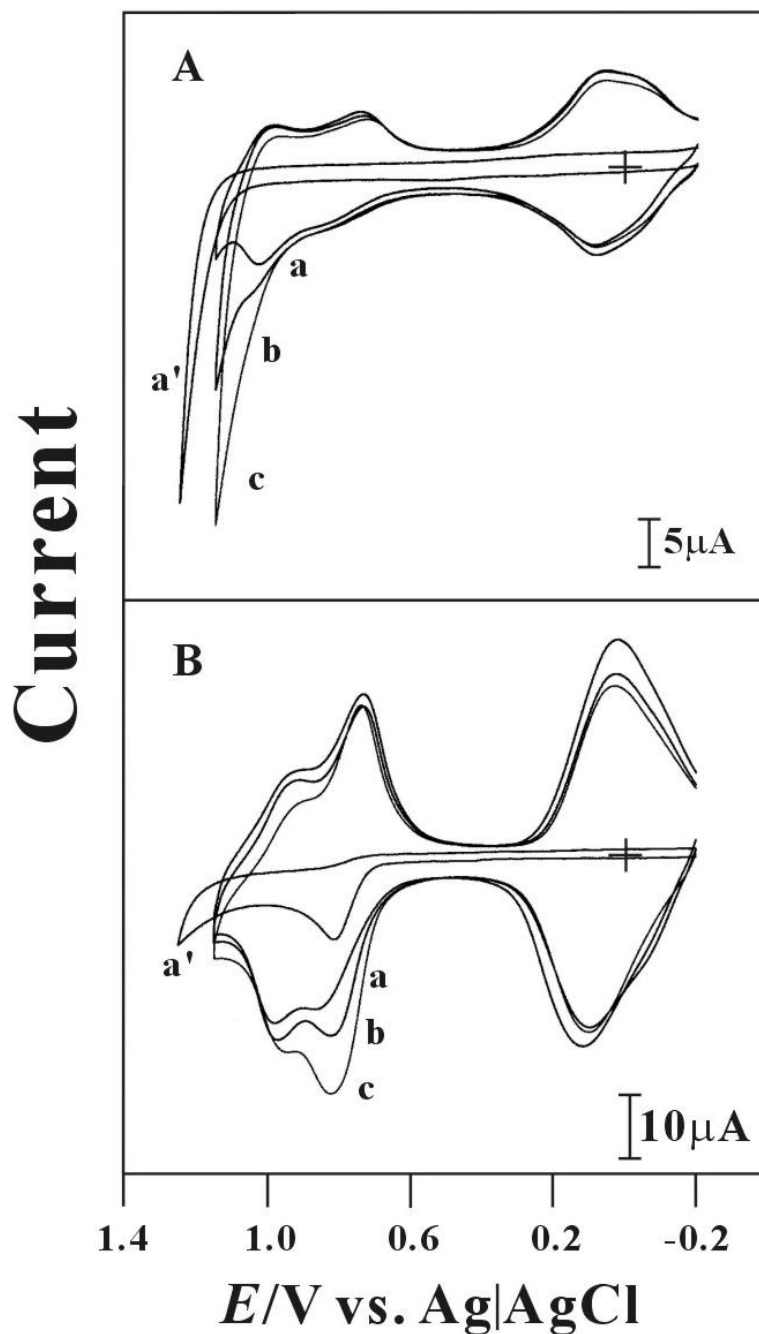
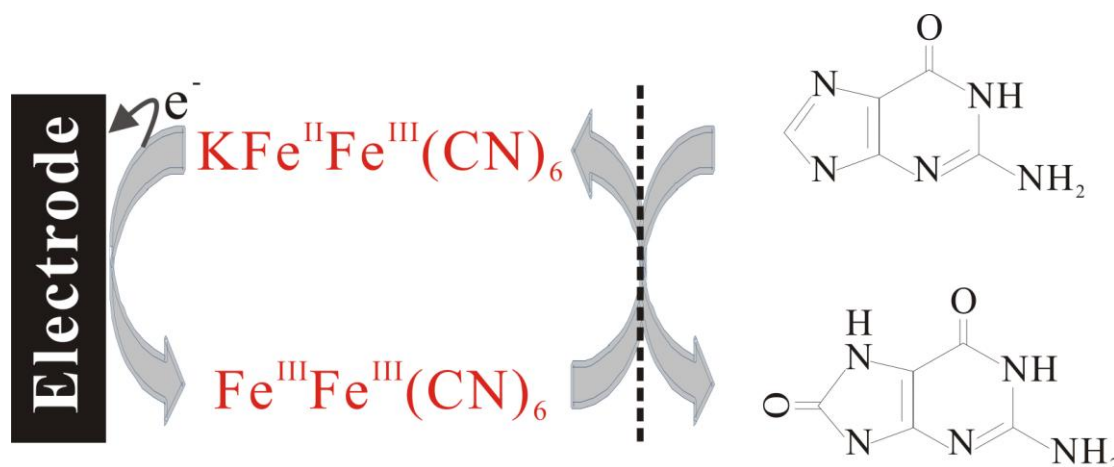


Figure 8. Cyclic voltammograms of FeHCF/GCE examined in 0.1 M NaCl aqueous solution with: (A) [adenine] = (a) 0, (b) 1×10^{-3} , (c) 2×10^{-3} M; and (B) [guanine] = (a) 0, (b) 1.5×10^{-3} , and (c) 3×10^{-3} M, respectively. (a') Cyclic voltammogram of bare GCE examined with maximal reagent addition in each case. Scan rate = 0.1 V s^{-1} .

The stability of FeHCF depended upon the pH of the aqueous solution. An acceptable stability of FeHCF was only achieved in acidic solution. So, the electrocatalytic oxidation of guanine and adenine by FeHCF films were investigated in acidic solutions (pH 6) containing KCl and NaCl, respectively. Fig. 7 showed the cyclic voltammograms of FeHCF film in an aqueous KCl solution (pH 6) in the presence of guanine or adenine. The electrocatalytic oxidation peak was found at +0.95 V and

+1.15 V for guanine and adenine, respectively. The anodic peak current increased while its cathodic peak current decreased, as the increase of guanine and adenine concentration. Compared with bare electrode, the modified electrode showed the higher current response and lower over-potential for these species. This means that the FeHCF composite was electro-active to guanine and adenine[50-51]. The electrocatalytic oxidation of guanine by FeHCF can be expressed as Scheme 1.



Scheme 1. Electrocatalytic oxidation of Guanine by FeHCF film.

The electrocatalytic oxidation of guanine and adenine in different supporting electrolyte was also studied by FeHCF film. It was carried out in 0.1 M NaCl aqueous solution (pH 6). Fig. 8 showed the cyclic voltammograms of FeHCF film examined in 0.1 M NaCl solution (pH 6) in the presence of adenine or guanine. It showed almost the same electrocatalytic oxidation peak at about +1.05 V for adenine. Particularly, two electrocatalytic oxidation peaks were found at +0.82 V and +0.98 V for guanine. The new anodic peak current increased at about +0.82 V similar to the oxidation peak of guanine using a bare glassy carbon electrode. However, it still showed the higher electrocatalytic oxidation current than bare electrode. One can conclude that FeHCF modified electrode was electro-active to adenine and guanine in both K^+ and Na^+ system.

3.5. Electrocatalytic oxidation of guanine and adenine mixture by cyclic voltammetry and amperometric determination of guanine

Simultaneously determination of adenine and guanine was studied by cyclic voltammetry and amperometry. Fig. 9A showed the voltammograms of FeHCF examined in 0.1 M KCl (pH 6) containing adenine and guanine. The electrocatalytic oxidation peaks were found at about +0.95 V and +1.25 V for oxidation of guanine and adenine, respectively.

The determination of guanine was further studied by amperometry using FeHCF film modified glassy carbon electrode. Fig. 9B showed a typical amperometric response for the determination of guanine with electrode rotation speed of 1500 rpm and applied potential of +0.85V. It exhibited good current response for 11 sequential additions of 1.3×10^{-6} M guanine. It showed a detection limit of 1 μA

(S/N = 3) and the current response showed a linear relationship with the concentration of guanine over the range of 0–145 μM and a sensitivity of $1818 \mu\text{A mM}^{-1} \text{cm}^{-2}$. These results indicated that the FeHCF can be a good catalyst used for good and accurate determination of guanine.

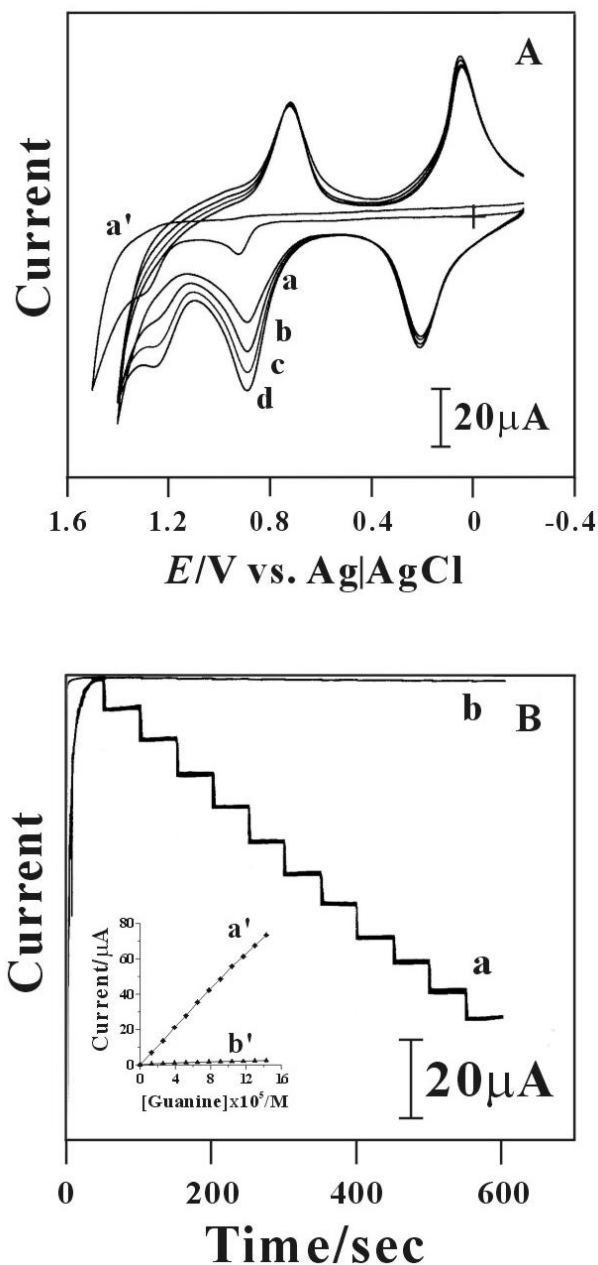


Figure 9. (A) Cyclic voltammograms of FeHCF/GCE examined in 0.1 M KCl aqueous solution with: [guanine] + [adenine] = (a) 0, (b) $1 \times 10^{-3} + 1 \times 10^{-3}$, (c) $2 \times 10^{-2} + 2 \times 10^{-2}$, and (d) $3 \times 10^{-3} + 3 \times 10^{-3}$ M. (a') Cyclic voltammogram of bare GCE examined with maximal reagent addition in this case. (B) Amperometric responses of 11 sequential additions of guanine (each 1.3×10^{-6} M) at (a) disk modified with iron(III) hexacyanoferrate film, (b) bare disk glassy carbon. Inset: Plot of the catalytic current vs. [guanine] at (a') disk modified with iron(III) hexacyanoferrate film, (b') bare disk glassy carbon. Here we used a GC disk electrode with a diameter of 6.02 mm, the electrode potential (E_{app}) and electrode rotation speed (ω) was set at $E_{\text{app}} = +0.85\text{V}$ and $\omega = 1500$ rpm, respectively.

3.6. Electrocatalytic oxidation of NADH and dopamine by FeHCF film

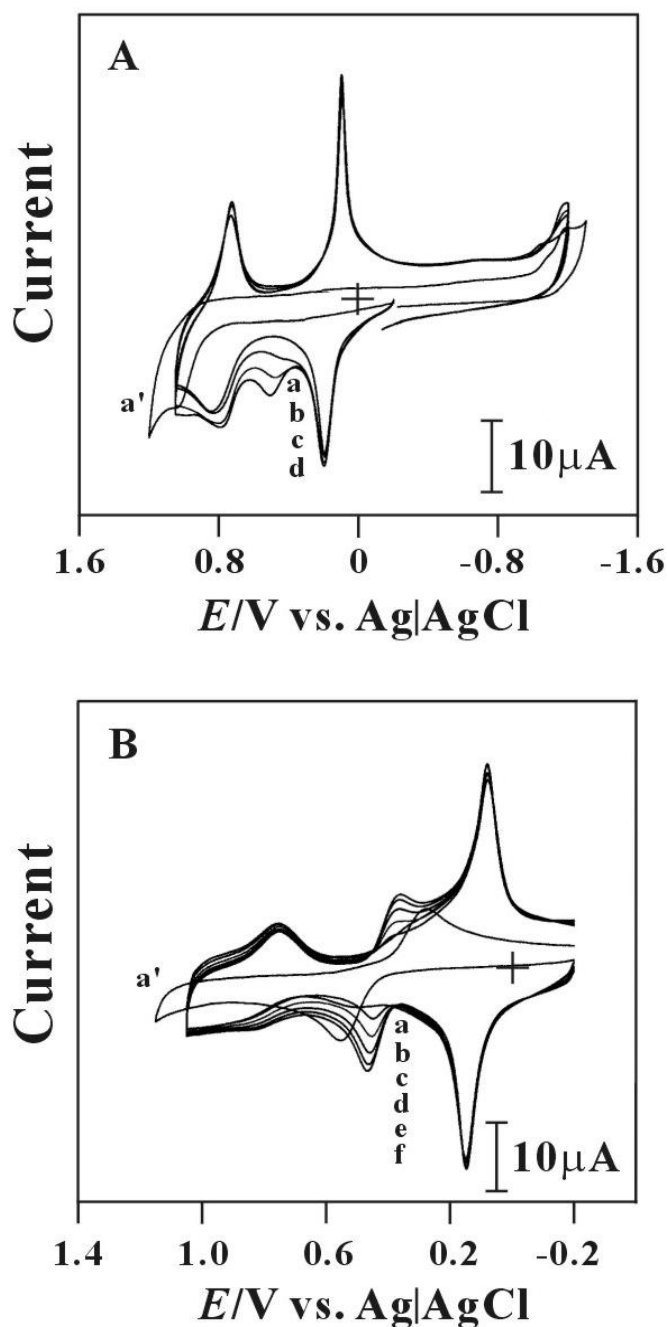


Figure 10. Cyclic voltammograms of FeHCF/GCE examined in: (A) 0.1 M KCl at pH 4 with [NADH] = (a) 0, (b) 5×10^{-4} , (c) 1×10^{-3} , (d) 1.5×10^{-3} M; and (B) 0.1 M KCl at pH 2 with [Dopamine] = (a) 2.5×10^{-4} , (b) 5×10^{-4} , (c) 7.5×10^{-4} , (d) 1×10^{-3} , (e) 1.25×10^{-3} , and (f) 1.5×10^{-3} M, respectively. (a') Cyclic voltammogram of bare GCE examined with maximal reagent addition in each case. Scan rate = 0.1 V s^{-1} .

The electrocatalytic oxidation of NADH and dopamine were also studied by FeHCF film modified electrode. Fig. 10A & B showed the cyclic voltammograms of FeHCF film examined with NADH and dopamine in 0.1 M KCl solution (pH 4). The electrocatalytic oxidation peak was found at

+0.5 V and +0.45 V for NADH and dopamine, respectively. This means that it has different electrocatalytic property to these species.

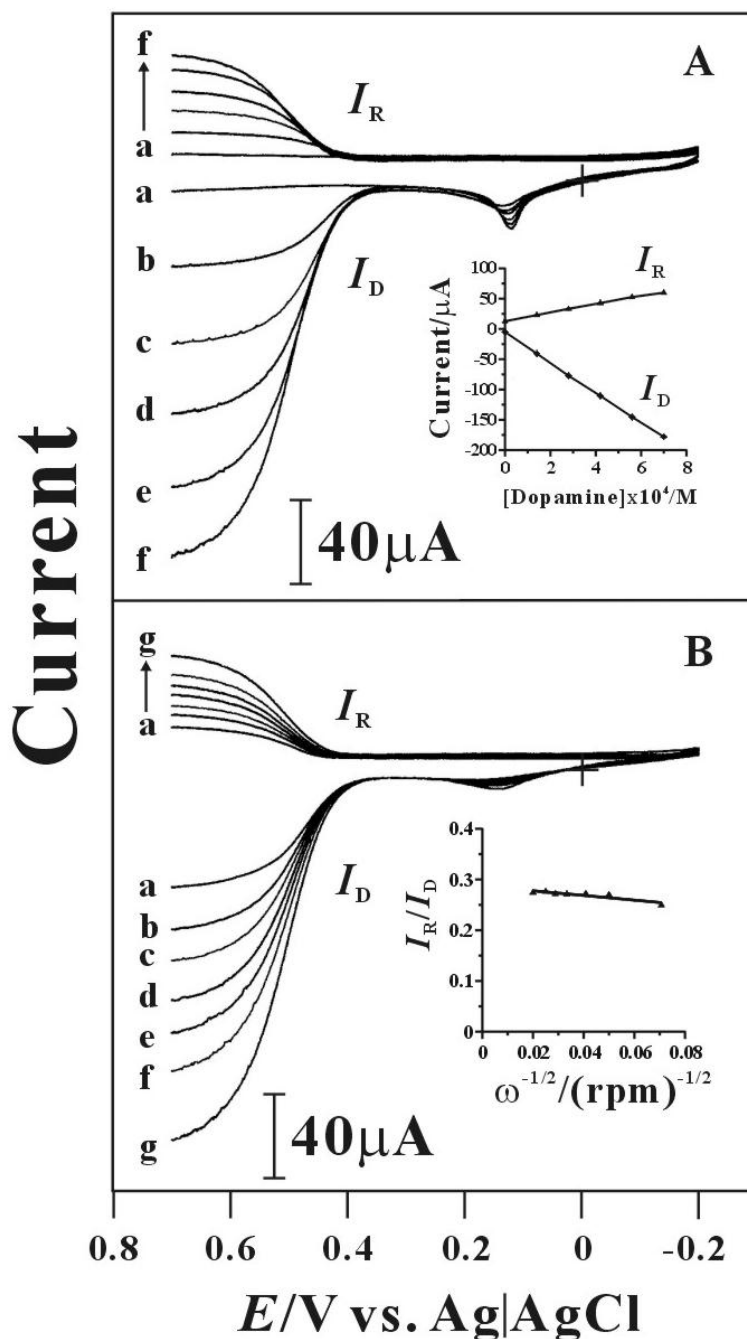


Figure 11. (A) RRDE voltammogram of an iron(III) hexacyanoferrate film adsorbed on a GC disk electrode with differing concentrations of dopamine in a 0.1 M KCl at pH 2. [Dopamine] = (a) 0, (b) 1.2×10^{-4} , (c) 2.4×10^{-4} , (d) 3.6×10^{-4} , (e) 4.8×10^{-4} and (f) 6×10^{-4} M, respectively. Electrode rotation speed = 2500 rpm; ring electrode applied potential at $E_R = 0$ V. Inset: a plot of electrode current (I_R and I_D) vs. [Dopamine]. (B) RRDE voltammogram of an iron(III) hexacyanoferrate film adsorbed on a GC disk electrode in 0.1 M KCl (pH 2) with different rotation rates: (a) 200, (b) 400, (c) 600, (d) 900, (e) 1200, (f) 1600, and (g) 2500 rpm, [dopamine] = 6×10^{-4} M. Inset: the plot of I_R/I_D vs. ω^{-1} . Scan rate = 0.015 V s^{-1} .

The electrocatalytic oxidation of NADH performed at the FeHCF film electrode involving the transfer of two electrons and one proton in the reaction as following equation:



The electrocatalytic oxidation and reversible reduction of dopamine by FeHCF film in an acidic aqueous solution is described by the following chemical reaction [52]:

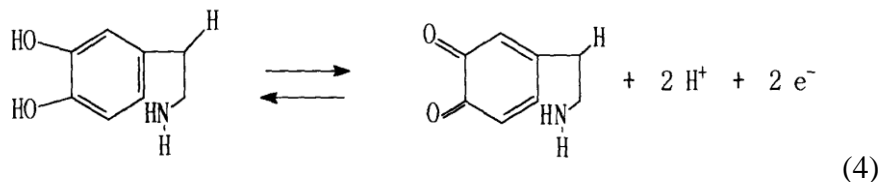


Fig. 11 showed the electrocatalytic oxidation of dopamine by FeHCF film using the rotating ring-disk electrode (RRDE) method with electrode rotation speed of 2500 rpm. Fig. 11A showed voltammetric response for dopamine with different concentration in 0.1 M KCl (pH 2) using FeHCF film modified disk-glassy carbon electrode. The ring-glassy carbon electrode applied potential of 0 V to reduce the NAD^+ formed from the product of disk electrode. The disk current (I_D) was obtained from the oxidation of NADH and the ring current (I_R) was obtained from the reduction of NAD^+ . These values (I_D & I_R) were directly proportional to dopamine concentration (as shown in the inset of Fig. 11A). They were consistent with the I_R current being the reduction current shown in equation (4).

Fig. 11B showed the voltammograms of FeHCF modified electrode examined with various rotation rates of 200-2500 rpm in 0.1 M KCl solution (pH 2) containing 6×10^{-4} M dopamine. The ring electrode applied potential of 0 V with scan rate of 0.015 V s^{-1} . These results were also consistent with I_D being the oxidation current and I_R being the reduction current described in Equation (4). The collection efficiency ($N = I_R/I_D$) was estimated for various rotation rates and the plot of I_R/I_D versus $\omega^{-1/2}$ was almost constant with an average value close to $N = 0.27$ (for $E_R = 0 \text{ V}$). It means that the collection efficiency of this electrode can be maintained in the range of electrode rotation speed.

3.7. The electrocatalytic reaction of H_2O_2 , L-cysteine, N_2H_4 , and NH_2OH by FeHCF film

The electrocatalytic reaction of H_2O_2 , L-cysteine, N_2H_4 , and NH_2OH were investigated by FeHCF film modified electrode in 0.1 M KCl (pH 4).

Fig. 12A showed the cyclic voltammograms of FeHCF/GCE examined in 0.1 M KCl solution (pH 4) containing H_2O_2 . The electrocatalytic reduction peak occurred at about +0.08 V and current increased as the increase of H_2O_2 concentration.

The electrocatalytic oxidation of L-cysteine, N_2H_4 , and NH_2OH by FeHCF film in 0.1 M KCl solution (pH 4) were obtained in Fig. 12C-D. The electrocatalytic oxidation peak was found at about +0.85 V, +0.95 V, and +0.9 V, respectively. The electrocatalytic oxidation of various substrates by FeHCF film is summarized in Table 1. By the results, one can know that the two redox couples of FeHCF are electro-active to various species.

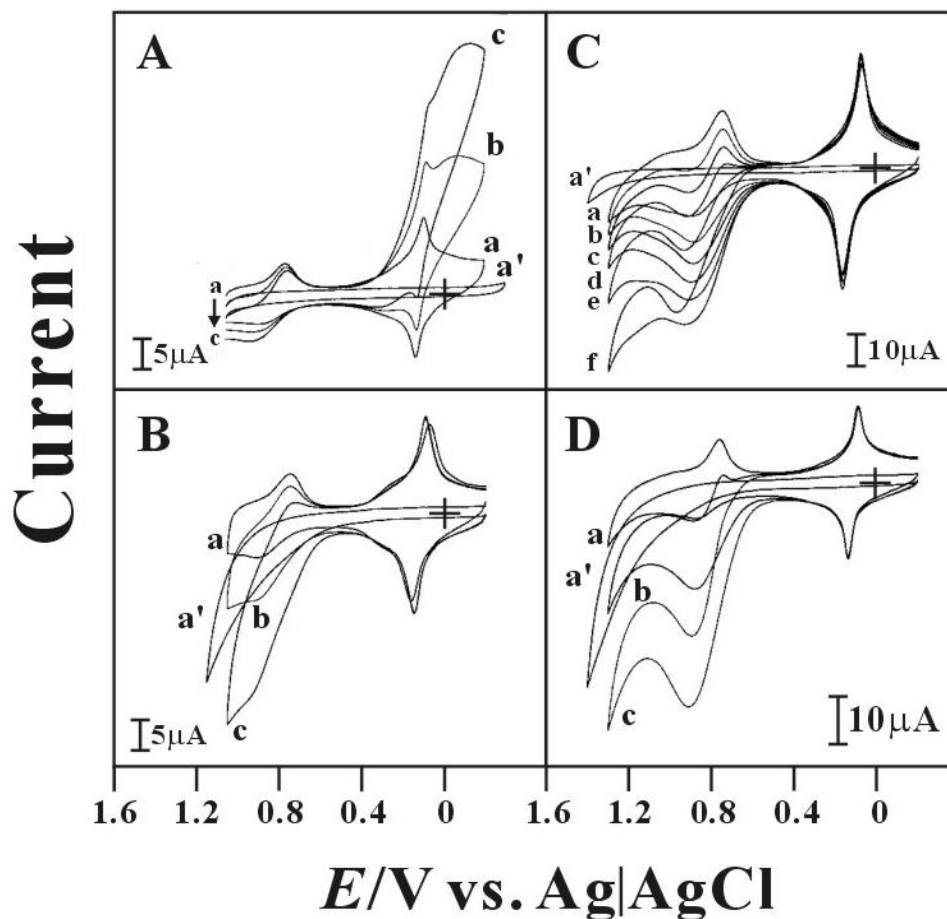


Figure 12. Cyclic voltammograms of FeHCF/GCE in 0.1 M KCl at pH 4 with: (A) $[\text{H}_2\text{O}_2] =$ (a) 0, (b) 2×10^{-2} , (c) 4×10^{-2} M; (B) $[\text{L-cysteine}] =$ (a) 0, (b) 2×10^{-3} , (c) 4×10^{-3} M; and (C) $[\text{N}_2\text{H}_4] =$ (a) 0, (b) 5×10^{-4} , (c) 1×10^{-3} , (d) 1.5×10^{-3} , (e) 2×10^{-3} , (f) 2.5×10^{-3} M; and (D) $[\text{NH}_2\text{OH}] =$ (a) 0, (b) 1×10^{-3} , and (c) 2×10^{-3} M, respectively. (a') Cyclic voltammogram of bare GCE examined with maximal reagent addition in each case. Scan rate = 0.1 V s^{-1} .

Table 1. The electrocatalytic properties of FeHCF film with various substrates.

Substrate	Electrocatalytic Reaction Type	Electrocatalytic Peak Potential, $E_{p,cat}^a / \text{V}$ (vs. Ag/AgCl)
Guanine	Oxidation (pH 6, KCl)	+0.95
Guanine	Oxidation (pH 6, NaCl)	+0.98, +0.8
Adenine	Oxidation (pH 6, KCl)	+1.15
Adenine	Oxidation (pH 6, NaCl)	+1.05
L-cysteine	Oxidation (pH 4, KCl)	+0.95
N_2H_4	Oxidation (pH 4, KCl)	+0.90
NH_2OH	Oxidation (pH 4, KCl)	+0.90
NADH	Oxidation (pH 4, KCl)	+0.55
Dopamine	Oxidation (pH 2, KCl)	+0.45
H_2O_2	Reduction (pH 4, KCl)	+0.08

^a $E_{p,cat}$: the anodic peak potential when substrate is added.

4. CONCLUSIONS

FeHCF film was successfully synthesized on electrode using consecutive cyclic voltammetry. It exhibited significant voltammograms with different supporting electrolyte including K^+ and Na^+ cations. In situ film growth and ion exchange effect of FeHCF film was characterized. FeHCF was confined to the surface, confirming the stability in neutral to acidic solution. It can electrocatalytically oxidize guanine, adenine and their mixture with different electrocatalytic property when carried out in K^+ and Na^+ solution. It was electro-active in the electrocatalytic oxidation of NADH, dopamine, L-cysteine, N_2H_4 , and NH_2OH as well as the electrocatalytic reduction of H_2O_2 .

ACKNOWLEDGEMENTS

This work was supported by the National Science Council of Taiwan (ROC).

References

1. E. Palecek, *Nature* 188 (1960) 656–657.
2. E. Palecek, *Electroanalysis* 8 (1996) 7–14.
3. C.J. Burrows, J.G. Muller, *Chem. Rev.* 98 (1998) 1109–1152.
4. S. Steenken, *Chem. Rev.* 89 (1989) 503–520.
5. A.C. Ontko, P.M. Armistead, S.R. Kircus, H.H. Thorp, *Inorg. Chem.* 38 (1999) 1842–1846.
6. J. Wang, S. Bollo, J.L.L. Paz, E. Sahlin, B. Mukherjee, *Anal. Chem.* 71 (1999) 1910–1913.
7. H.H. Thorp, *Trends Biotechnol.* 16 (1998) 117–121
8. J. Wang, *Chem. Eur. J.* 5 (1999) 1681–1685.
9. E. Palecek, M. Fojta, *Anal. Chem.* 73 (2001) 74A–83A.
10. E.E. Ferapontova, *Electrochim. Acta* 49 (2004) 1751–1759.
11. A.M. Oliveira-Brett, L.A. Silva, C.M.A. Brett, *Langmuir* 18 (2002) 2326–2330.
12. A. Abbaspour, M.A. Mehrgardi, R. Kia, *J. Electroanal. Chem.* 568 (2004) 261–266.
13. N.A. El-Maali, J. Wang, *Sens. Actuators B* 76 (2001) 211–214.
14. J.M. Zen, M.R. Chang, G. Ilangovan, *Analyst* 124 (1999) 679–684.
15. D.H. Johnson, K.C. Glasgow, H.H. Thorp, *J. Am. Chem. Soc.* 117 (1995) 8933–8938.
16. R.C. Holmberg, H.H. Thorp, *Anal. Chem.* 75 (2003) 1851–1860.
17. K.M. Millan, A.J. Spurmanis, S.R. Mikkelsen, *Electroanalysis* 4 (1992) 929–932.
18. J. Wang, X. Cai, G. Rivas, H. Shiraishi, P.A.M. Farias, N. Dontha, *Anal. Chem.* 68 (1996) 2629–2634.
19. H. Kouri-Yousoufi, F. Garnier, P. Srivasta, A. Yassar, *J. Am. Chem. Soc.* 119 (1997) 7388–7389.
20. T. M. Herne, M. J. Tarlov, *J. Am. Chem. Soc.* 119 (1997) 8916–8920.
21. Z. Wang, S. Xiao, Y. Chen, *J. Electroanal. Chem.* 589 (2006) 237–242
22. J. Wang, X. Cai, C. Jonsson, M. Balakrishnan, *Electroanalysis* 8 (1996) 20–24.
23. J. Wang, J.R. Fernandes, L.T. Kubota, *Anal. Chem.* 70 (1998) 3699–3702.
24. P. Singhal, K.T. Kawagoe, C.N. Christian, W.G. Kuhr, *Anal. Chem.* 69 (1997) 1662–1668.
25. P. Singhal, W.G. Kuhr, *Anal. Chem.* 69 (1997) 4828–4832.
26. A. Abbaspour, A. Ghaffarinejad, *Electrochim. Acta* 53 (2008) 6643–6650.
27. L. M. Siperko, T. Kuwana, *J. Electrochem. Soc.* 130 (1983) 396–402.
28. T. R. I. Cataldi, G. E. De Benedetto, *J. Electroanal. Chem.* 458 (1998) 149–154.
29. K. Honda, H. Hayashi, *J. Electrochem. Soc.* 134 (1987) 1330–1334.
30. K. Itaya, I. Uchida, V.D. Neff, *Acc. Chem. Res.* 19 (1986) 162–168.
31. D.N. Upadhyay, D.M. Kolb, *J. Electroanal. Chem.* 358 (1993) 317–325.

32. V. D. Neff, *J. Electrochem. Soc.* 132 (1985) 1382–1384.
33. R. J. Mortimer, D. R. Rosseinsky, *J. Chem. Soc. Dalton Trans.* (1984) 2059–2061.
34. T. H. Tsai, T. W. Chen, S. M. Chen, K. C. Lin, *Int. J. Electrochem. Sci.* 6 (2011) 2058 – 2071.
35. T. H. Tsai, Y. C. Huang, S. M. Chen, *Int. J. Electrochem. Sci.* 6 (2011) 3238 – 3253.
36. J.A. Cox, P.J. Kulesza, *Anal. Chem.* 56 (1984) 1021–1025.
37. K. Ogura, I. Yoshida, *Electrochim. Acta* 32 (1987) 1191–1197.
38. C. Lin, A. B. Bocarsly, *J. Electroanal. Chem.* 300 (1991) 325–345.
39. B. D. Humphrey, S. Sinha, A.B. Bocarsly, *J. Phys. Chem.* 91 (1987) 586–593.
40. P. J. Kulesza, K. Brajter, E. Dabek-Zlotorzynska, *Anal. Chem.* 59 (1987) 2776–2780.
41. S. M. Chen, *J. Electroanal. Chem.* 521 (2002) 29–52.
42. S. M. Chen, M. F. Lu, K. C. Lin, *J. Electroanal. Chem.* 579 (2005) 163–174.
43. S. M. Chen, *J. Electroanal. Chem.* 401 (1996) 147–154.
44. S. M. Chen, *Electrochim. Acta* 43 (1998) 3359–3369.
45. P. J. Kulesza, M. A. Malik, M. Berrettoni, M. Giorgetti, S. Zamponi, R. Schmidt, R. Marassi, *J. Phys. Chem. B* 102 (1998) 1870–1876.
46. S. J. Reddy, A. Dostal, F. Scholz, *J. Electroanal.chem.* 403 (1996) 209–212.
47. T. Garc'ia, E. Casero, E. Lorenzo, F. Pariente, *Sens. Actuators B* 106 (2005) 803–809.
48. S. M. Chen, J. L. Lin, *J. Electroanal. Chem.* 571 (2004) 223–232.
49. S. M. Chen, K. T. Peng, *J. Electroanal. Chem.* 547 (2003) 179–189.
50. S. M. Chen, C. H. Wang, *J. Solid State Electrochem.*, 11(2007) 581-591.
51. S. M. Chen, C. H. Wang, *Bioelectrochem.*, 70(2007) 452-461.
52. P. Hernandez, I. Sanchez, F. Paton, L. Hernandez, *Talanta* 46 (1998) 985–991.